Special Topics & Reviews in Porous Media — An International Journal, 10(3):203–223 (2019)

HEAT AND MASS TRANSFER ON FREE CONVECTIVE FLOW OF A MICROPOLAR FLUID THROUGH A POROUS SURFACE WITH INCLINED MAGNETIC FIELD AND HALL EFFECTS

M. Veera Krishna,[1,*] P.V.S. Anand,[1] & Ali J. Chamkha[2,3]

[1]*Department of Mathematics, Rayalaseema University, Kurnool, Andhra Pradesh 518007, India*
[2]*Department of Mechanical Engineering, Prince Sultan Endowment for Energy and Environment, Prince Mohammad Bin Fahd University Al-Khobar 31952, Kingdom of Saudi Arabia*
[3]*RAK Research and Innovation Center, American University of Ras Al Khaimah, 10021 United Arab Emirates*

*Address all correspondence to: M. Veera Krishna, Department of Mathematics, Rayalaseema University, Kurnool, Andhra Pradesh 518007, India; Tel.: +91 984 965 0682; Fax: +91 08 518 272 600, E-mail: veerakrishna_maths@yahoo.com

Original Manuscript Submitted: 6/15/2018; Final Draft Received: 10/10/2018

The effects of heat and mass transfer on free convective flow of micropolar fluid were studied over an infinite vertical porous plate in the presence of an inclined magnetic field with an angle of inclination α *with a constant suction velocity and taking Hall current into account. The dimensionless governing equations are reduced to a system of linear differential equations, making use of a regular perturbation method, and equations are solved analytically. The control of various parameters on the flow is discussed graphically. This present study is of immediate interest in geophysical, medicine, biology, and all those processes that are greatly embellished by a strong magnetic field with a low density of the gas. The resultant velocity trim downs with increasing suction parameter and viscosity ratio, while it enhances with heat source parameter. The micro-rotational velocity rises with increasing Hall parameter. The temperature increases with increasing heat radiation parameter and reduces with suction parameter. Concentration diminishes with increasing chemical reaction parameter. The rate of heat transfer increase with Prandtl number and the rate of mass transfer enhances with the chemical reaction parameter.*

KEY WORDS: *convection, Hall effects, heat transfer, MHD flows, micropolar fluids, porous media*

1. INTRODUCTION

Micropolar fluids contain microconstituents that can undergo rotation, which can affect the hydrodynamics of the flow that can be distinctly non-Newtonian. These fluids with microstructure belong to a class of complex fluids with nonsymmetrical stress tensors referred to as micro-orphic fluids. They have many practical applications, such as analyzing the behavior of exotic lubricants, the flow of colloidal suspensions or polymeric fluids, liquid crystals, additive suspensions, animal blood, body fluids, and turbulent shear flows.

Many investigators have studied micropolar fluids in external flows (Bhargava et al., 2010; Sarifuddin et al., 2013). The theory of micropolar fluids was developed by Eringen (1964, 1972). Comprehensive studies on micropolar fluids, thermo-micropolar fluids, and their applications in engineering and technology were presented by Ariman et al. (1973) and Prathap Kumar et al. (2010). Srinivasacharya et al. (2001) analyzed the unsteady stokes flow of micropolar fluid between two parallel porous plates. Muthuraj and Srinivas (2010) investigated fully developed

2151–4798/19/$35.00

NOMENCLATURE

(u, v, w)	velocity components along x, y, z directions (ms^{-1})
(x, y, z)	Cartesian co-ordinates (m)
(N_1, N_2)	micro-rotation components
C	concentration of solute (kgm^{-3})
C_w	concentration of solute at plate (kgm^{-3})
C_∞	concentration of solute far away from plate (kgm^{-3})
C_p	specific heat at constant pressure ($Jkg^{-1}K$)
C_s	couple stress coefficient
C_f	skin friction coefficient
D_m	molecular diffusivity (m^2s^{-1})
e	electron charge (C)
F	heat radiation parameter
g	acceleration due to gravity (ms^{-2})
Gr	thermal Grashof number
Gm	modified Grashof number
H_0	applied magnetic field (A/m)
H	strength of magnetic field (A/m)
i	imaginary unit
J	micro inertia density or current strength
K	permeability of porous medium (Darcy) (kgm^{-3})
k_1	thermal conductivity of fluid (W/m K)
$k*$	mean absorption coefficient
L	dimensionless material parameter
M	magnetic field parameter
m	Hall parameter
n	frequency of oscillation (Hertz)
n_e	number electron density (kgm^{-3})
Nu	Nusselt number
P_e	electron pressure (Nm^{-2})
Pr	Prandtl number
Q	additional heat source (kW/m^3)
Q_i	radiation absorption parameter
q	velocity vector (m/s)
q_r	radiative heat flux (P/A)
R	rotational parameter
Re_x	local Reynolds number
R_r	chemical reaction rate constant
S	suction parameter
Sc	Schmidt number
Sh_x	Sherwood number
T	temperature of fluid in boundary layer (K)
t	non-dimensional time (s)
T_w	wall temperature of fluid (K)
T_∞	temperature of fluid far away from plate (K)
U_r	uniform reference velocity (ms^{-1})
V	velocity vector (ms^{-1})
w_0	normal velocity (ms^{-1})

Greek Symbols

α	chemical reaction parameter
β_c	coefficient of concentration expansion (m^3kg^{-1})
β_T	coefficient of thermal expansion (K^{-1})
Δ	viscosity ratio
ε	small constant quantity
θ	non-dimensional temperature
Λ	spin gradient velocity ($m\ s^{-1}$)
μ	coefficient of viscosity ($N\ S\ m^{-2}$)
μ_e	magnetic permeability ($H\ m^{-1}$)
ν	coefficient of kinematic viscosity (m^2s^{-1})
ν_c	kinematic micro-rotation viscosity (m^2s^{-1})
ρ	density of fluid ($kg\ m^{-3}$)
σ	electrical conductivity of fluid ($s\ m^{-1}$)
σ^*	Stefan-Boltzmann constant parameter
τ_e	electron collision time (s)
ϕ	non-dimensional concentration
Ω	angular velocity ($m\ s^{-1}$)
ω_e	electron frequency (J)
ω	micro-rotation profile

Subscripts

w	condition at the wall
∞	condition at free stream

magnetohydrodynamic (MHD) flow of a micropolar and viscous fluid in a vertical porous space. The pioneering works of Hickman (1957) and Mazumder (1991) laid the foundation stone in this field. The flow and heat transfer in a rotating system with various physical situations were studied by Ezzat and Othman (2000), Ezzat et al. (1999), Chakraborti et al. (2005), and Othman et al. (2004, 2005). Damseh et al. (2009) studied the combined effect of heat generation or absorption and first order chemical reaction to micropolar fluid flows over a uniform stretched surface. Other related studies were described by Rahman and Al-Lawatia (2010), Rahman et al. (2010), and Sivaraj and Rushi Kumar (2012). In the above cited investigations, the effect of thermal radiation on the flow and heat transfer has not been provided.

Abo-Eldohad and Ghonaim (2005) analyzed the radiation effects on heat transfer of a micropolar fluid through a porous medium. Rahman and Sultana (2008) studied the steady convective flow of a micropolar fluid past a vertical porous flat plate in the presence of radiation with variable heat flux in porous medium. The effects of thermal radiation were also investigated by Mahmoud (2007) and Chamkha et al. (2011). The influence of a magnetic field on the flow of an electrically conducting viscous fluid with mass transfer and radiation absorption is also useful in planetary atmosphere research (Shercliff, 1965). Umavathi and Malashetty (2005) studied free convective flow in a vertical channel with symmetric and asymmetric boundary heating in the presence of viscous and Joulean dissipations. The effects of chemical reaction and radiation absorption in the unsteady MHD free convection flow past a semi-infinite vertical permeable moving plate with a heat source and suction were analyzed by Ibrahim et al. (2008) and Sudheer Babu and Satya Narayana (2009).

Applications in biomedical engineering include cardiac MRI and ECG. Engineering applications in areas of Hall accelerators as well as in flight MHD were studied by Hayat et al. (2007), Rani and Tomar (2010), Satya Narayana et al. (2011, 2013), and Ahmed and Kalita (2011). Bakr (2011) presented an analysis of MHD free convection and mass transfer adjacent to moving vertical plate for micropolar fluid in a rotating frame of reference in the presence of heat generation/absorption and a chemical reaction. The same study was extended by Das (2011) with thermal radiation effects. To the best of our knowledge, the problem of MHD unsteady free convection flow of a micropolar fluid in a rotating frame of reference to Hall effects and radiation absorption has remained unexplored.

Veera Krishna and Gangadhar Reddy (2018) discussed the unsteady MHD free convection in a boundary layer flow of an electrically conducting fluid through porous medium subject to uniform transverse magnetic field over a moving infinite vertical plate in the presence of heat source and chemical reaction. Veera Krishna and Subba Reddy (2018a) have investigated the simulation on the MHD forced convective flow through stumpy permeable porous medium (oil sands, sand) using a Lattice Boltzmann method. Veera Krishna and Jyothi (2018a) discussed the Hall effects on MHD rotating flow of a visco-elastic fluid through a porous medium over an infinite oscillating porous plate with heat source and chemical reaction. Reddy et al. (2018) investigated MHD flow of viscous incompressible nano-fluid through a saturating porous medium. Veera Krishna and Swarnalathamma (2016), Swarnalathamma and Veera Krishna (2016), Veera Krishna and Gangadhar Reddy (2016), and Veera Krishna and Subba Reddy (2016) discussed the MHD flows of an incompressible and electrically conducting fluid in planar channel. Veera Krishna et al. (2018a) analyzed heat and mass transfer on unsteady MHD oscillatory flow of blood through porous arterioles. The effects of radiation and Hall current on an unsteady MHD free convective flow in a vertical channel filled with a porous medium were studied by Veera Krishna et al. (2018b). The heat generation/absorption and thermo-diffusion on an unsteady free convective MHD flow of radiating and chemically reactive second grade fluid near an infinite vertical plate through a porous medium and taking the Hall current into account were studied by Veera Krishna and Chamkha (2018). Veera Krishna et al. (2018c) discussed the heat and mass transfer on unsteady, MHD oscillatory flow of second-grade fluid through a porous medium between two vertical plates under the influence of fluctuating heat source/sink, and chemical reaction. Veera Krishna et al. (2018d) investigated the heat and mass transfer on MHD free convective flow over an infinite non-conducting vertical flat porous plate. Veera Krishna and Jyothi (2018b) discussed the effect of heat and mass transfer on free convective rotating flow of a visco-elastic incompressible electrically conducting fluid past a vertical porous plate with time dependent oscillatory permeability and suction in presence of a uniform transverse magnetic field and heat source. Veera Krishna and Subba Reddy (2018b) investigated the transient MHD flow of a reactive second grade fluid through a porous medium between two infinitely long horizontal parallel plates. Veera Krishna et al. (2018e) discussed heat and mass-transfer effects on an unsteady flow of a chemically reacting micropolar fluid over an infinite vertical porous plate in the presence of an inclined magnetic field, Hall current effect, accounting for thermal radiation taken. Veera Krishna et al. (2010) discussed Hall effects on steady hydromagnetic flow of a couple stress fluid through a composite medium in a rotating parallel plate channel with porous bed on the lower half. Veera Krishna et al. (2018f) discussed the heat and mass transfer on non-linear MHD flow through oscillating infinite vertical porous surface. Veera Krishna et al. (2018g) investigated the heat and mass transfer on MHD flow of second grade fluid through porous medium over a semi-infinite vertical stretching sheet.

A comprehensive study of laminar natural convection heat transfer around cylinders of elliptical cross section wrapped with a porous medium is conducted by Mohsen et al. (2017). The porous blunt nosecone transpiration cooling process under supersonic incoming flow conditions using a two-domain approach based on the preconditioned density-based algorithm was studied by Wu et al. (2017). Profile modification is an efficient method used by Fu (2018) to improve the areal sweep efficiency of water flooding. The problem of thermal instability was investigated by Kaothekar (2018) for partially ionized thermal plasma, which has a connection in astrophysical condensations and is responsible for formation of objects in an astrophysical plasma environment.

MHD boundary layer flow and heat transfer of a viscous incompressible fluid over a radiative stretching cylinder with variable thermal conductivity embedded in a porous medium was discussed by Kalpana and Gupta (2018). Sravan and Rushi (2018) studied the fascinating and novel characteristics of MHD convective nanofluid over a stretching sheet through a porous medium.

We report here the effects of heat and mass transfer on free convective flow of micropolar fluid over an infinite vertical porous plate in the presence of an inclined magnetic field with an angle of inclination α with a constant suction velocity and taking Hall current into account.

2. FORMULATION AND SOLUTION OF THE PROBLEM

We consider an unsteady three-dimensional free convective flow of micropolar fluid over an infinite vertical porous plate in the presence of an inclined magnetic field with an angle of inclination α with a constant suction velocity and accounting for Hall current. The flow is assumed to be in the x-direction, which is taken along the plate in upward direction, and the z-axis is normal to it and the y-axis along the width of the plate as shown in Fig. 1. The fluid is considered to be a gray, emitting, and absorbing heat, but a non-scattering medium.

When the strength the magnetic field is very large, the generalized Ohm's law is modified to include Hall current.

$$J + \frac{\omega_e \tau_e}{H_0} J \times H = \sigma(E + \mu_e q \times H) \tag{1}$$

In Eq. (1), the electron pressure gradient, the ion-slip and thermo-electric effects are neglected. We also assume that the electric field $E = 0$. Under these assumptions

$$J_x + mJ_z \sin\alpha = -\sigma\mu_e H_0 w \sin\alpha \tag{2}$$

$$J_z + mJ_x \sin\alpha = -\sigma\mu_e H_0 u \sin\alpha \tag{3}$$

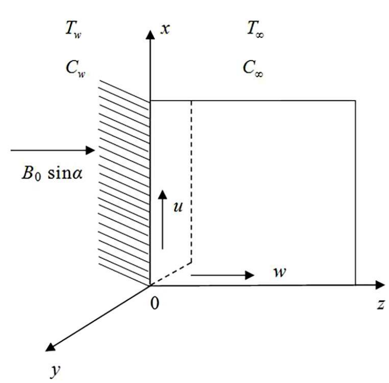

FIG. 1: Physical configuration of problem

where $m = \omega_e \tau_e$ is the Hall parameter. On solving Eq. (2) and (3), we obtain:

$$J_x = \frac{\sigma \mu_e H_0 \sin\alpha}{1 + m^2 \sin^2\alpha} \left(um \sin\alpha - w\right) \tag{4}$$

$$J_z = \frac{\sigma \mu_e H_0 \sin\alpha}{1 + m^2 \sin^2\alpha} \left(u + wm \sin\alpha\right) \tag{5}$$

The following assumptions are made:

1. All the fluid properties except the density in the buoyancy force are constant.
2. The plate is electrically non-conducting.
3. The magnetic Reynolds number is so small that the induced magnetic field can be neglected. Also, the electrical conductivity σ of the fluid is reasonably low, and hence the Ohmic dissipation may be neglected.
4. It is assumed that there is no applied voltage, which implies that the electric field is absent.

The equations governing the flow heat and mass transfer are:

$$\frac{\partial w}{\partial z} = 0 \tag{6}$$

$$\frac{\partial u}{\partial t} + w\frac{\partial u}{\partial z} = (\nu + \nu_r)\frac{\partial^2 u}{\partial z^2} - \nu_r \frac{\partial N_2}{\partial z} + \frac{\sigma \mu_e^2 H_0^2 \sin^2\alpha \left(m \sin\alpha \nu - u\right)}{\rho\left(1 + m^2 \sin^2\alpha\right)} - \frac{\nu}{k}u + g\beta_T \left(T - T_\infty\right) + g\beta_C \left(C - C_\infty\right) \tag{7}$$

$$\frac{\partial w}{\partial t} + w\frac{\partial w}{\partial z} = (\nu + \nu_r)\frac{\partial^2 w}{\partial z^2} - \nu_r \frac{\partial N_1}{\partial z} - \frac{\sigma \mu_e^2 H_0^2 \sin^2\alpha \left(m \sin\alpha u + w\right)}{\rho\left(1 + m^2 \sin^2\alpha\right)} - \frac{\nu}{k}w \tag{8}$$

$$\frac{\partial N_1}{\partial t} + w\frac{\partial N_1}{\partial z} = \frac{\Lambda}{\rho j}\frac{\partial^2 N_1}{\partial z^2} \tag{9}$$

$$\frac{\partial N_2}{\partial t} + w\frac{\partial N_2}{\partial z} = \frac{\Lambda}{\rho j}\frac{\partial^2 N_2}{\partial z^2} \tag{10}$$

$$\frac{\partial T}{\partial t} + w\frac{\partial T}{\partial z} = \frac{k_1}{\rho C_p}\frac{\partial^2 T}{\partial z^2} - \frac{Q}{\rho C_p}\left(T - T_\infty\right) + \frac{Q_1^*}{\rho C_p}\left(C - C_\infty\right) - \frac{1}{\rho C_p}\frac{\partial q_r}{\partial z} \tag{11}$$

$$\frac{\partial C}{\partial t} + w\frac{\partial C}{\partial z} = D_m \frac{\partial^2 C}{\partial z^2} - R_r\left(C - C_\infty\right) \tag{12}$$

The relevant boundary conditions are:

$$\begin{gathered} u = w = 0, \quad N_1 = N_2 = 0, \quad T = T_\infty, \quad C = C_\infty \quad \text{for} \quad t \leq 0 \\ u = U_r\left\{1 + \frac{\varepsilon}{2}\left(e^{int} + e^{-int}\right)\right\}, \quad w = 0 \end{gathered} \tag{13}$$

$$N_1 = -\frac{1}{2}\frac{\partial v}{\partial z}, \quad N_2 = \frac{1}{2}\frac{\partial u}{\partial z}, \quad T = T_w, \quad C = C_w, \quad \text{at} \quad z = 0, \quad \text{for} \quad t > 0 \tag{14}$$

$$u = w = 0, \quad N_1 = N_2 = 0, \quad T = T_\infty, \quad C = C_\infty \quad \text{as} \quad z \to \infty \tag{15}$$

The oscillatory plate velocity assumed in Eq. (14) is based on the suggestion proposed by Ganapathy (1994). We now consider a convenient solution of the continuity equation (6) to be

$$w = -w_0 \tag{16}$$

where w_0 represents the normal velocity at the plate, which is positive for suction and negative for blowing. The radiative heat flux term by using the Rosseland approximation is given by

$$q_r = -\frac{4\sigma^*}{3k^*}\frac{\partial T^4}{\partial z} \tag{17}$$

$$T^4 = 4TT_\infty^3 - 3T_\infty^4 \tag{18}$$

$$\frac{\partial q_r}{\partial z} = -\frac{16T_\infty^3\sigma^*}{3k^*}\frac{\partial^2 T}{\partial z^2} \tag{19}$$

Let us introduced the following non-dimensional quantities:

$$u^* = \frac{u}{U},\quad w^* = \frac{w}{U_{r,}},\quad z^* = \frac{zU_r}{\nu},\quad t^* = \frac{tU_r^2}{\nu},\quad n^* = \frac{n\nu}{U_r^2},\quad Q_1 = \frac{Q_1^*\left(C_w - C_\infty\right)}{\left(T_w - T_\infty\right)U_r^2}$$

$$N_1^* = \frac{N_1\nu}{U_r^2},\quad N_2^* = \frac{N_2\nu}{U_r^2},\quad Kc = \frac{R_r\nu}{U_r^2},\quad M = \frac{\mu_e H_0}{U_r}\sqrt{\frac{\sigma\nu}{\rho}},\quad L = \frac{\Lambda}{\mu j},\quad \Delta = \frac{\nu_r}{\nu},\quad K = \frac{kU_r^2}{\nu^2}$$

$$F = \frac{4T_\infty^3\sigma}{k_1k^*},\quad S = \frac{w_0}{U_r},\quad \mathrm{Sc} = \frac{\nu}{D_m},\quad \mathrm{Pr} = \frac{\mu C_p}{k},\quad \theta = \frac{T - T_\infty}{T_w - T_\infty},\quad \phi = \frac{C - C_\infty}{C_w - C_\infty}$$

$$\mathrm{Gr} = \frac{\nu g\beta_T\left(T_w - T_\infty\right)}{U_r^3},\quad \mathrm{Gm} = \frac{\nu g\beta_T\left(C_w - C_\infty\right)}{U_r^3},\quad Q^* = \frac{Q\nu^2}{U_r^2k}$$

In view of Eq. (19), the basic field Eqs. (6)–(12) can be expressed in non-dimensional form as:

$$\frac{\partial u}{\partial t} - S\frac{\partial u}{\partial z} = \left(1+\Delta\right)\frac{\partial^2 u}{\partial z^2} - \Delta\frac{\partial N_2}{\partial z} - \left(\frac{M^2\sin^2\alpha}{1+m^2\sin^2\alpha} + \frac{1}{K}\right)u + \left(\frac{mM^2\sin^3\alpha}{1+m^2\sin^2\alpha}\right)w + \mathrm{Gr}\theta + \mathrm{Gm}\phi \tag{20}$$

$$\frac{\partial w}{\partial t} - S\frac{\partial w}{\partial z} = \left(1+\Delta\right)\frac{\partial^2 w}{\partial z^2} + \Delta\frac{\partial N_1}{\partial z} - \left(\frac{M^2\sin^2\alpha}{1+m^2\sin^2\alpha} + \frac{1}{K}\right)w - \left(\frac{mM^2\sin^3\alpha}{1+m^2\sin^2\alpha}\right)u \tag{21}$$

$$\frac{\partial N_1}{\partial t} - S\frac{\partial N_1}{\partial t} = L\frac{\partial^2 N_1}{\partial z^2} \tag{22}$$

$$\frac{\partial N_2}{\partial t} - S\frac{\partial N_2}{\partial t} = L\frac{\partial^2 N_2}{\partial z^2} \tag{23}$$

$$\frac{\partial\theta}{\partial t} - S\frac{\partial\theta}{\partial z} = \frac{1}{\mathrm{Pr}}\left(1 + \frac{4F}{3}\right)\frac{\partial^2\theta}{\partial z^2} - \frac{Q}{\mathrm{Pr}}\theta + Q_1\phi \tag{24}$$

$$\frac{\partial\phi}{\partial t} - S\frac{\partial\phi}{\partial z} = \frac{1}{Sc}\frac{\partial^2\phi}{\partial z^2} - Kc\phi \tag{25}$$

The corresponding boundary conditions (13) and (14) in view of scaling relation (20) reduce to

$$u = w = 0,\quad N_1 = N_2 = 0,\quad \theta = 0,\quad \phi = 0\quad \text{for}\quad t \le 0 \tag{26}$$

$$\begin{gathered} u = 1 + \frac{\varepsilon}{2}\left(e^{int} + e^{-int}\right),\quad w = 0,\quad N_1 = -\frac{1}{2}\frac{\partial w}{\partial z},\quad N_2 = \frac{1}{2}\frac{\partial u}{\partial z},\quad \theta = 1,\quad \phi = 1,\quad \text{as}\quad z = 0 \\ u = w = 0,\quad N_1 = N_2 = 0,\quad \theta = 0,\quad \phi = 0,\quad \text{as}\quad z \to \infty \end{gathered} \tag{27}$$

To obtain desired solutions, we now simplify Eqs. (22)–(25) by putting the fluid velocity and angular velocity in the complex form as:

$$V = u + iw\quad \text{and}\quad \omega = N_1 + iN_2$$

we get

$$\frac{\partial V}{\partial t} - S\frac{\partial V}{\partial z} = (1+\Delta)\frac{\partial^2 V}{\partial z^2} + i\Delta\frac{\partial \omega}{\partial z} - \left(\frac{M^2\sin^2\alpha}{1+m^2\sin^2\alpha} + \frac{1}{K}\right)V - i\left(\frac{mM^2\sin^3\alpha}{1+m^2\sin^2\alpha}\right)V + \text{Gr}\theta + \text{Gm}\phi \quad (28)$$

$$\frac{\partial \omega}{\partial t} - S\frac{\partial \omega}{\partial z} = L\frac{\partial^2 \omega}{\partial z^2} \quad (29)$$

The associated boundary condition (28) and (29) become

$$V = 0,\quad \omega = 0,\quad \theta = 0,\quad \phi = 0 \quad \text{for} \quad t \le 0 \quad (30)$$

$$\begin{aligned} V = 1 + \frac{\varepsilon}{2}(e^{int} + e^{-int}),\quad \omega = \frac{i}{2}\frac{\partial V}{\partial z},\quad \theta = 1,\quad \phi = 1 \quad \text{at} \quad z = 0, \\ V = 0,\quad \omega = 0,\quad \theta = 0,\quad \phi = 0,\quad \text{as} \quad z \to \infty,\quad \text{for} \quad t > 0 \end{aligned} \quad (31)$$

In order to reduce the above system of partial differential equations in dimensionless form, we may represent the linear and angular velocities, temperature, and concentration as V, ω, θ, and ϕ as

$$\left.\begin{aligned} V(z,t) = V_0 + \frac{\varepsilon}{2}\left\{e^{int}V_1(z) + e^{-int}V_2(z)\right\},\quad \omega(z,t) = \omega_0 + \frac{\varepsilon}{2}\left\{e^{int}\omega_1(z) + e^{-int}\omega_2(z)\right\} \\ \theta(z,t) = \theta_0 + \frac{\varepsilon}{2}\left\{e^{int}\theta_1(z) + e^{-int}\theta_2(z)\right\},\quad \phi(z,t) = \phi_0 + \frac{\varepsilon}{2}\left\{e^{int}\phi_1(z) + e^{-int}\phi_2(z)\right\} \end{aligned}\right\} \quad (32)$$

Substituting the above Eq. (32) into the Eqs. (22), (23), (25), and (27) and equating the harmonic and nonharmonic terms and neglecting the higher order terms $O(\varepsilon^2)$, we obtain the following set of equations:

Zeroth order equations are:

$$(1+\Delta)V_0'' + SV_0' - a_1V_0 + \text{Gr}\theta_0 + \text{Gm}\phi_0 + i\Delta\omega_0' = 0 \quad (33)$$

$$L\omega_0'' + S\omega_0' = 0 \quad (34)$$

$$(3+4F)\theta_0'' + 3S\text{Pr}\theta_0' - 3Q\theta_0 + 3Q_1\text{Pr}\phi_0 = 0 \quad (35)$$

$$\phi_0'' + S\text{Sc}\phi_0' - Kc\text{Sc}\phi_0 = 0 \quad (36)$$

First order equations are:

$$(1+\Delta)V_1'' + SV_1' - a_2V_1 + \text{Gr}\theta_1 + \text{Gm}\phi_1 + i\Delta\omega_1' = 0 \quad (37)$$

$$L\omega_1'' + S\omega_1' - in\omega_1 = 0 \quad (38)$$

$$(3+4F)\theta_1'' + 3S\text{Pr}\theta_1' - 3(Q + in\text{Pr})\theta_1 + 3Q_1\text{Pr}\phi_1 = 0 \quad (39)$$

$$\phi_1'' + S\text{Sc}\phi_1' - (Kc + in)\phi_1 = 0 \quad (40)$$

Second order equations are:

$$(1+\Delta)V_2'' + SV_2' - a_3V_2 + \text{Gr}\theta_2 + \text{Gm}\phi_2 + i\Delta\omega_2' = 0 \quad (41)$$

$$L\omega_2'' + S\omega_2' + in\omega_2 = 0 \quad (42)$$

$$(3+4\text{F})\theta_2'' + 3S\text{Pr}\theta_2' - 3(Q - in\text{Pr})\theta_2 + 3Q_1\text{Pr}\phi_2 = 0 \quad (43)$$

$$\phi_2'' + S\text{Sc}\phi_2' - (Kc - in)\phi_2 = 0 \quad (44)$$

where the prime denote differentiation with respect to z the corresponding boundary conditions can be written as

$$\begin{aligned} V_0 = V_1 = V_2 = 1,\quad \omega_0 = \frac{i}{2}V_0',\quad \omega_1 = \frac{i}{2}V_1',\quad \omega_2 = \frac{i}{2}V_1' \\ \theta_0 = 1,\quad \theta_1 = \theta_2 = 0,\quad \phi_0 = 1,\quad \phi_1 = \phi_2 = 0,\quad \text{at} \quad z = 0 \end{aligned} \quad (45)$$

$$V_0 = V_1 = V_2 = 0, \quad \omega_0 = \omega_1 = \omega_2 = 0$$
$$\theta_0 = 1, \quad \theta_1 = \theta_2 = 0, \quad \phi_0 = 1, \quad \phi_1 = \phi_2 = 0, \quad \text{at} \quad z \to \infty \tag{46}$$

Solving Eqs. (33)–(43) under the boundary conditions (45) and (46), we obtain the expressions for translation velocity, micro-rotation, temperature, and concentrations as:

$$V = A_3 e^{-m_1 z} + A_4 e^{-m_2 z} + A_5 e^{-m_3 z} + A_6 e^{-(S/L)z} + \frac{\varepsilon}{2}\left\{\left(A_7 e^{-m_4 z} + A_8 e^{-m_5 z}\right) e^{int} + \left(A_8 e^{-m_6 z} + A_{10} e^{-m_7 z}\right) e^{int}\right\} \tag{47}$$

$$\omega = B_1 e^{-(S/L)z} + \frac{\varepsilon}{2}\left\{B_2 e^{int - m_4 z} + B_3 e^{-int + m_6 z}\right\} \tag{48}$$

$$\theta = A_1 e^{-m_1 z} + A_2 e^{-m_2 z} \tag{49}$$

$$\phi = e^{-m_1 z} \tag{50}$$

The physical quantities of engineering interest are skin friction coefficient, couple stress coefficient number, and Sherwood number. The skin friction is caused by viscous drag in the boundary layer around the plate, and then it is important to discuss the skin friction from the knowledge of velocity. Free skin friction non-dimensional form can be calculated as follows:

$$C_f = \frac{\tau_{\omega|z=0}}{\rho U_r^2} = \left\{1 + \Delta\left(1 + \frac{i}{2}\right)\right\} V'(0) = -\left\{1 + \Delta\left(1 + \frac{i}{2}\right)\right\} \times \left[A_3 m_1 + A_4 m_2 + A_5 m_3 + \frac{S}{L} A_6 + \frac{\varepsilon}{2}\left\{\left(A_7 m_4 + A_8 m_5\right) e^{int} + \left(A_9 m_6 + A_{10} m_7\right) e^{int}\right\}\right] \tag{51}$$

The couple stress coefficient at the wall C_s is given by:

$$C_s = \left.\frac{\partial \omega_1}{\partial z}\right|_{z=0} + i \left.\frac{\partial \omega_2}{\partial z}\right|_{z=0} = \omega'(0) = -\left\{\frac{SB_1}{L} + \frac{\varepsilon}{2}\left(B_2 m_4 e^{int} + B_3 m_6 e^{-int}\right)\right\} \tag{52}$$

The rate of heat transfer between the fluid and the plate is studied through non-dimensional Nusselt number. The rate of heat transfer in terms of Nusselt number is given by:

$$\text{Nu} = \frac{\chi\left[(\partial T)/(\partial z)\right]_{z=0}}{T_w - T_\infty} = -\text{Re}_x \theta'(0) \Rightarrow \frac{\text{Nu}}{\text{Re}_x} = -\theta'(0) = A_1 m_1 + A_2 m_2 \tag{53}$$

where $\text{Re}_x = (U_r x)/\nu$ is the local Reynolds number.

The local Sherwood number Sh_x is given by

$$\text{Sh}_x = -\frac{\chi\left[(\partial C)/(\partial z)\right]_{z=0}}{C_w - C_\infty} = -\text{Re}_x \phi'(0) \Rightarrow \frac{\text{Sh}_x}{\text{Re}_x} = -\phi'(0) = m_1 \tag{54}$$

where

$$a_1 = \left(\frac{M^2 \sin^2\alpha}{1 + m^2 \sin^2\alpha} + \frac{1}{K}\right) + i\left(\frac{mM^2 \sin^3\alpha}{1 + m^2 \sin^3\alpha}\right)$$
$$a_2 = \left(\frac{M^2 \sin^2\alpha}{1 + m^2 \sin^2\alpha} + \frac{1}{K}\right) + i\left(n + \frac{mM^2 \sin^3\alpha}{1 + m^2 \sin^3\alpha}\right)$$
$$a_3 = \left(\frac{M^2 \sin^2\alpha}{1 + m^2 \sin^2\alpha} + \frac{1}{K}\right) + i\left(-n + \frac{mM^2 \sin^3\alpha}{1 + m^2 \sin^2\alpha}\right)$$
$$m_1 = \frac{SSc + \sqrt{(SSc)^2 + 4KcSc}}{2}, \quad m_2 = \frac{3S\text{Pr} + \sqrt{(3S\text{Pr})^2 + 12Q(3 + 4F)}}{2(3 + 4F)},$$
$$m_3 = \frac{S + \sqrt{S^2 + 4a_1(1 + \Delta)}}{2(1 + \Delta)}, \quad m_4 = \frac{S + \sqrt{S^2 + 4inL}}{2L}, \quad m_5 = \frac{S + \sqrt{S^2 + 4a_2(1 + \Delta)}}{2(1 + \Delta)},$$

$$m_6 = \frac{S + \sqrt{S^2 - 4inL}}{2L}, \quad m_7 = \frac{S + \sqrt{S^2 + 4a_3\left(1 + \Delta\right)}}{2\left(1 + \Delta\right)}$$

$$A_1 = \frac{-3Q_1 \mathrm{Pr}}{\left(3 + 4F\right) m_1^2 - 3S\mathrm{Pr} m_1 - 3Q}, \quad A_2 = 1 - A_1,$$

$$A_3 = \frac{-\left(Gm + GrA_1\right)}{\left(1 + \Delta\right) m_1^2 - Sm_1 - a_1}, \quad A_4 = \frac{-GmA_2}{\left(1 + \Delta\right) m_2^2 - Sm_2 - a_1}, \quad A_5 = 1 - A_3 - A_4 - A_6,$$

$$A_6 = \frac{\Delta SL\left\{A_3\left(m_1 - m_3\right) + A_4\left(m_2 - m_3\right) + m_3\right\}}{\left(2 + \Delta\right) S^2 - 2L\left(S^2 + La_1\right) + \Delta SLm_3}, \quad A_7 = \frac{\Delta m_4 m_5}{\left(2 + \Delta\right) m_4^2 - 2\left(Sm_4 + a_2\right) + \Delta m_4 m_3},$$

$$A_8 = 1 - A_7, \quad A_9 = \frac{\Delta m_6 m_7}{\left(2 + \Delta\right) m_6^2 - 2\left(Sm_6 + a_3\right) + \Delta m_6 m_7}, \quad \text{and} \quad A_{10} = 1 - A_9$$

$$B_1 = \frac{i\left\{A_3\left(m_3 - m_1\right) + A_4\left(m_2 - m_3\right) - m_3\right\}\left\{\left(1 + \Delta\right) S^2 - LS^2 - a_1 L^2\right\}}{\left(2 + \Delta\right) S^2 - 2L\left(S^2 + La_1\right) + \Delta SLm_3}$$

$$B_2 = \frac{im_5\left\{\left(1 + \Delta\right) m_4^2 - Sm_4 - a_2\right\}}{\left(2 + \Delta\right) m_4^2 - 2\left(Sm_4 + a_2\right) + \Delta m_4 m_5}, \quad B_3 = \frac{im_7\left\{\left(1 + \Delta\right) m_6^2 - Sm_6 - a_3\right\}}{\left(2 + \Delta\right) m_6^2 - 2\left(Sm_6 + a_3\right) + \Delta m_6 m_7}$$

3. RESULTS AND DISCUSSION

The flow was governed by the nonparameters M, magnetic field parameter; m, hall parameter; K, permeability parameter; Prandtl number, Pr; the angle of inclination, α; Kc, chemical reaction parameter; Gr, thermal Grashof number; Gm, modified Grashof number; Sc, Schmidt parameter; n, frequency of oscillation; Δ, viscosity ratio; S, suction parameter; F, heat radiation parameter; Q, additional heat source; and Q_1, radiation absorption parameter; Numerical evaluation of analytical results reported in the previous section was performed, and a representative set of results is reported graphically in Figs. 2–20. They represent the velocity, microrotation, temperature, and concentration profiles with respect to the governing parameters, while other parameters are varied over a range that are listed in figure captions.

Figure 2 represents the primary and secondary velocity profiles for different values of a magnetic field parameter M. Both the velocity components decrease with increase in a magnetic field parameter M along the surface. These effects are much stronger near the surface of the plate. This indicates that the fluid velocity reduced by increasing the magnetic field, and confirms that the application of a magnetic field to an electrically conducting fluid produces a dragline force that causes reduction in the fluid velocity. This remarkable feature of the velocity profiles in our investigation is due to the presence of transverse magnetic field, Hall current, and radiation absorption in the flow

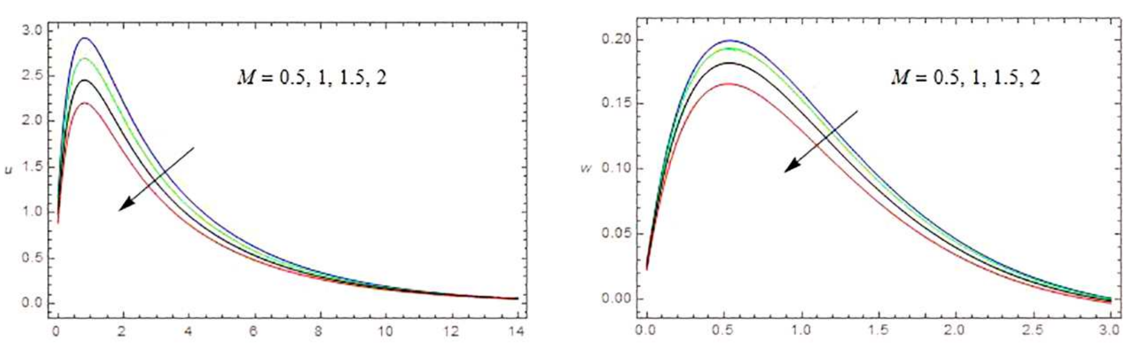

FIG. 2: Velocity profiles against M with $K = 0.5$, $m = 1$, $\mathrm{Pr} = 0.71$, $\alpha = \pi/6$, $Kc = 1$, $\mathrm{Gr} = 3$, $\mathrm{Gm} = 2$, $\mathrm{Sc} = 0.22$, $n = \pi/6$, $\Delta = 0.1$, $S = 1$, $F = 0.2$, $Q = 1$, $Q_1 = 0.2$

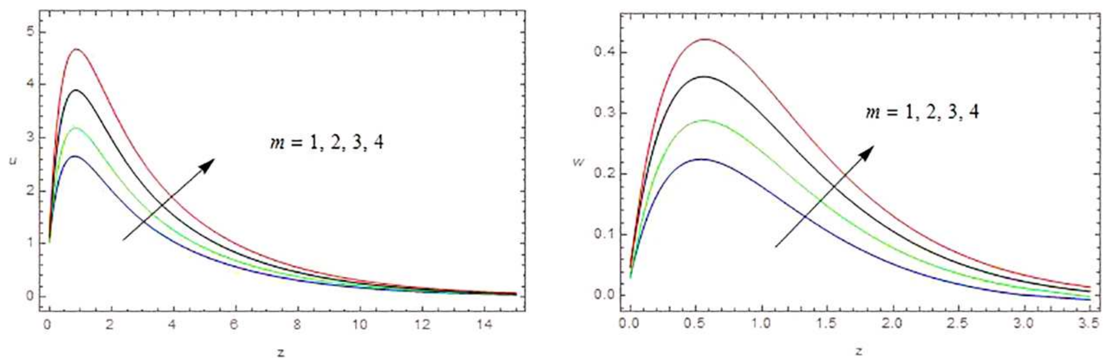

FIG. 3: Velocity profiles against m with $M = 0.5$, $K = 0.5$, Pr $= 0.71$, $\alpha = \pi/6$, $Kc = 1$, Gr $= 3$, Gm $= 2$, Sc $= 0.22$, $n = \pi/6$, $\Delta = 0.1$, $S = 1$, $F = 0.2$, $Q = 1$, $Q_1 = 0.2$

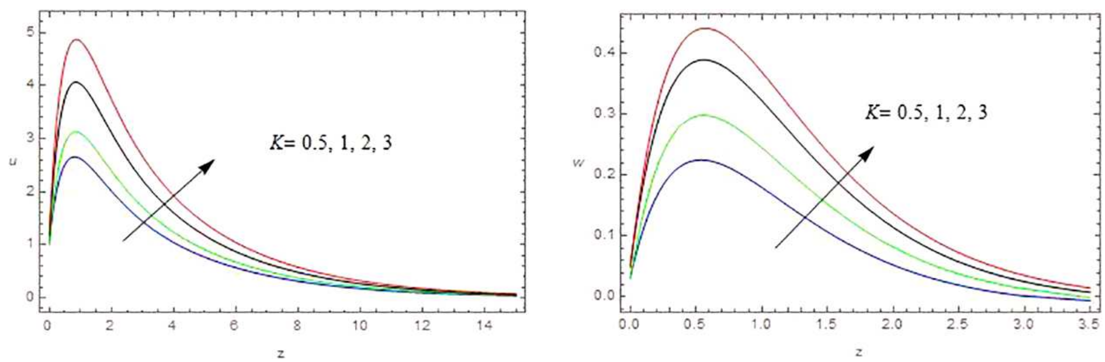

FIG. 4: Velocity profiles against K with $M = 0.5$, $m = 1$, Pr $= 0.71$, $\alpha = \pi/6$, $Kc = 1$, Gr $= 3$, Gm $= 2$, Sc $= 0.22$, $n = \pi/6$, $\Delta = 0.1$, $S = 1$, $F = 0.2$, $Q = 1$, $Q_1 = 0.2$

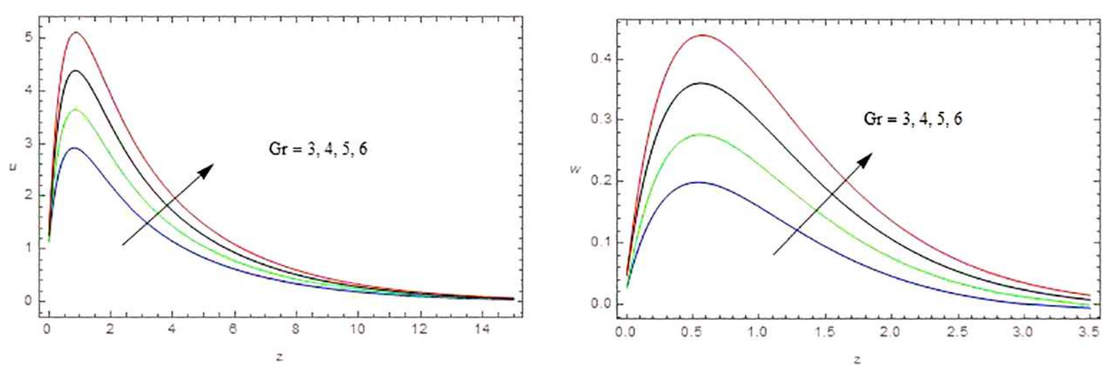

FIG. 5: Velocity profiles against Gr with $M = 0.5$, $K = 0.5$, $m = 1$, Pr $= 0.71$, $\alpha = \pi/6$, $Kc = 1$, Gm $= 2$, Sc $= 0.22$, $n = \pi/6$, $\Delta = 0.1$, $S = 1$, $F = 0.2$, $Q = 1$, $Q_1 = 0.2$

field. This phenomenon has a good agreement with the physical realities. Both velocity components u and w increase with an increased Hall parameter m (Fig. 3).

Similar behavior is observed with increased permeability parameter K (Fig. 4). Here particularly we observed that lower the permeability, the lesser the fluid speed in the entire fluid region. Figures 5, 6, and 8 reveal that both the velocity components enhance with increasing thermal Grashof number Gr, mass Grashof number Gm, and additional heat source Q. We also observed that the velocity component u reduces and the secondary velocity increases with increasing frequency of oscillation n (Fig. 7). Figure 9 shows that the primary and secondary velocity components u

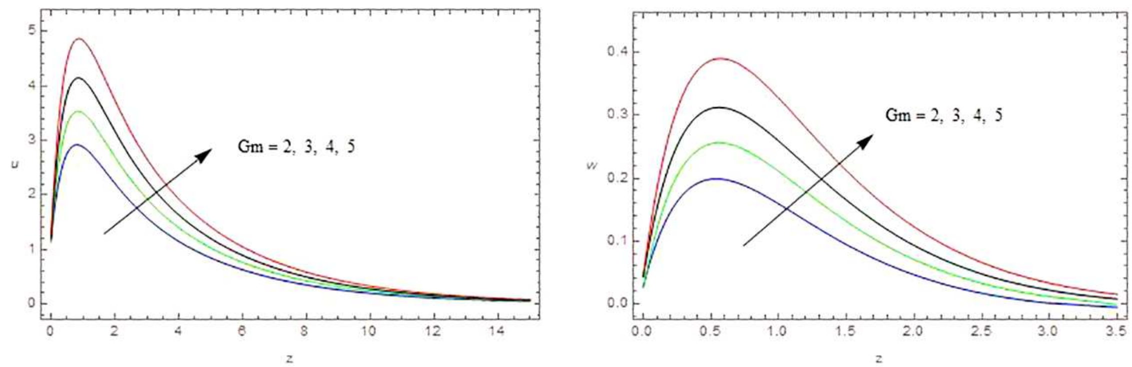

FIG. 6: Velocity profiles against Gm with $M = 0.5$, $K = 0.5$, $m = 1$, Pr $= 0.71$, $\alpha = \pi/6$, $Kc = 1$, Gr $= 3$, Sc $= 0.22$, $n = \pi/6$, $\Delta = 0.1$, $S = 1$, $F = 0.2$, $Q = 1$, $Q_1 = 0.2$

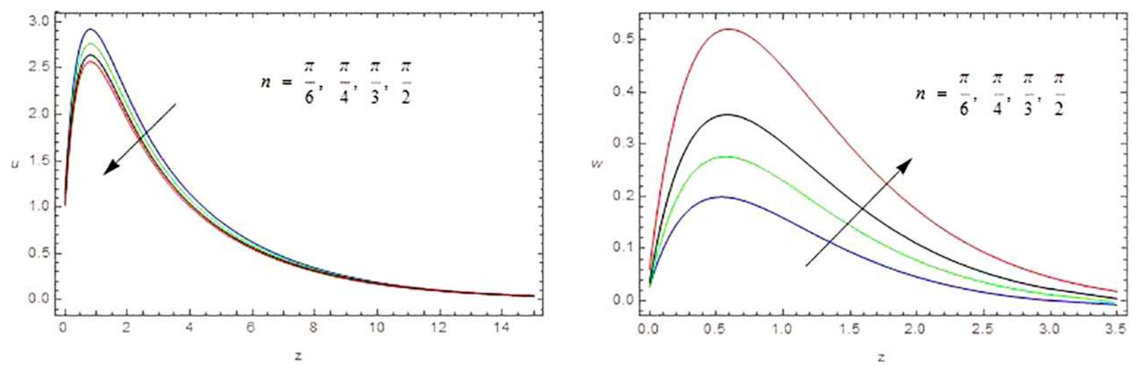

FIG. 7: Velocity profiles against n with $M = 0.5$, $K = 0.5$, $m = 1$, Pr $= 0.71$, $\alpha = \pi/6$, $Kc = 1$, Gr $= 3$, Gm $= 2$, Sc $= 0.22$, $\Delta = 0.1$, $S = 1$, $F = 0.2$, $Q = 1$, $Q_1 = 0.2$

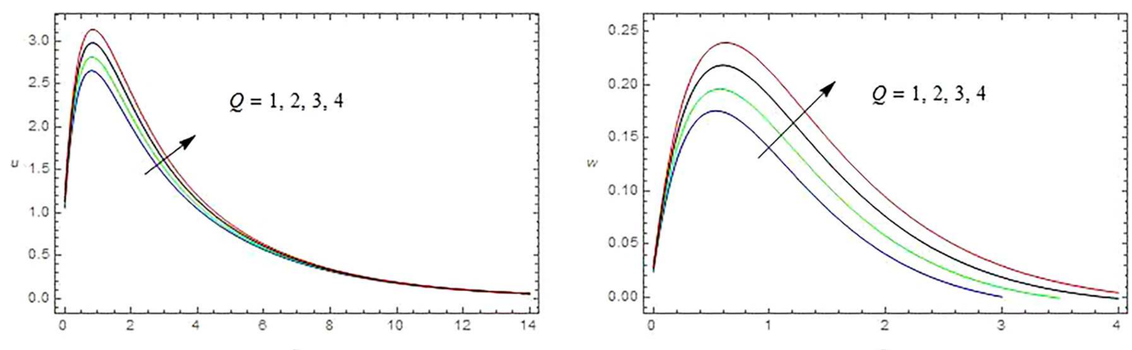

FIG. 8: The velocity profiles against Q with $M = 0.5$, $K = 0.5$, $m = 1$, Pr $= 0.71$, $\alpha = \pi/6$, $Kc = 1$, Gr $= 3$, Gm $= 2$, Sc $= 0.22$, $n = \pi/6$, $\Delta = 0.1$, $S = 1$, $F = 0.2$, $Q_1 = 0.2$

and w reduce with increasing radiation absorption parameter Q_1 throughout the fluid medium. Finally, the velocity components u and w decrease with increasing the angle of inclination α (Fig. 10).

The micro-rotation profiles for N_1 are negative because the micro-rotation of the fluid is anti-clockwise. Figure 11 depicts the micro-rotational velocity profiles for N_1 and N_2 with different values of magnetic field parameter M. The micro-rotational velocity distribution for N_1 increase and N_2 decrease with an increase in the magnetic field parameter (Hartmann number) throughout the fluid region. Figure 12 illustrates the micro-rotational velocity distribution for different values of Hall parameter m. As Hall current parameter m increases, micro-rotational velocity components

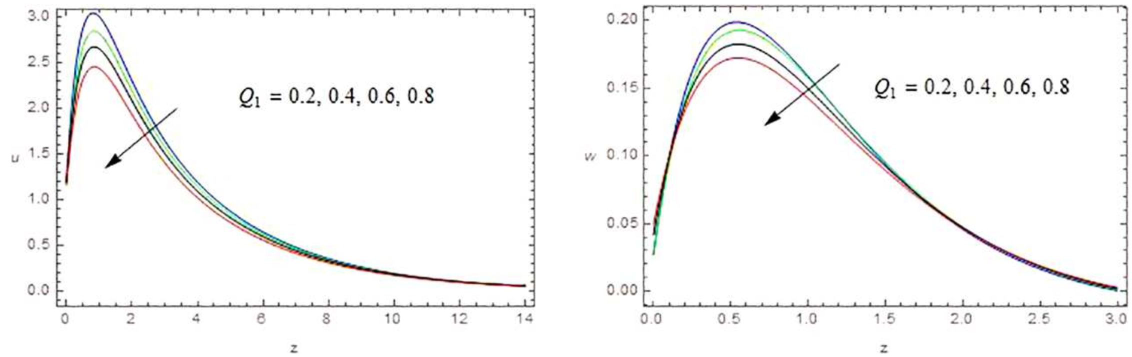

FIG. 9: Velocity profiles against Q_1 with $M = 0.5$, $K = 0.5$, $m = 1$, Pr $= 0.71$, $\alpha = \pi/6$, $Kc = 1$, Gr $= 3$, Gm $= 2$, Sc $= 0.22$, $n = \pi/6$, $\Delta = 0.1$, $S = 1$, $F = 0.2$, $Q = 1$

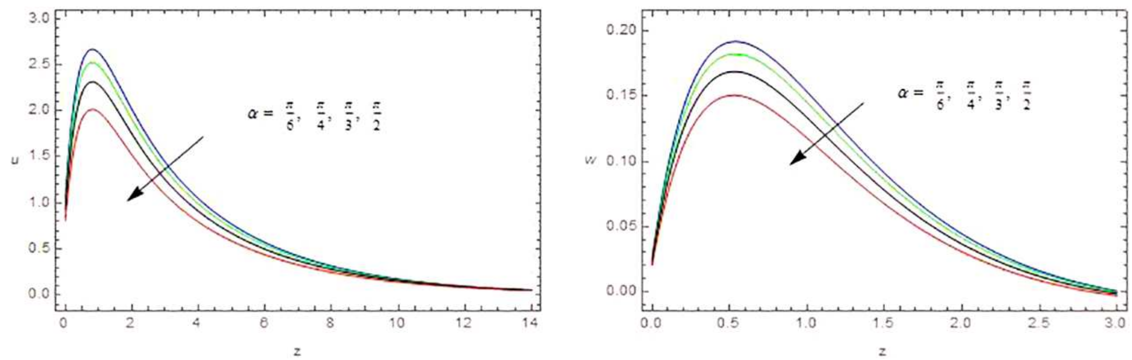

FIG. 10: Velocity profiles against α with $M = 0.5$, $K = 0.5$, $m = 1$, Pr $= 0.71$, $Kc = 1$, Gr $= 3$, Gm $= 2$, Sc $= 0.22$, $n = \pi/6$, $\Delta = 0.1$, $S = 1$, $F = 0.2$, $Q = 1$, $Q_1 = 0.2$

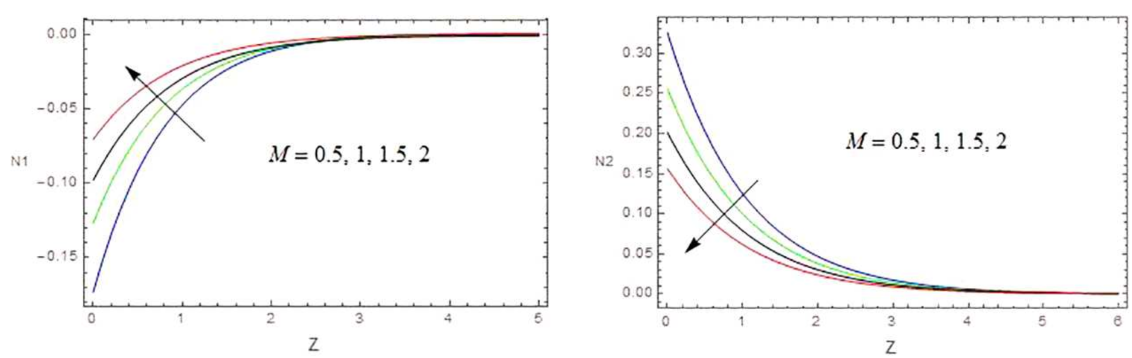

FIG. 11: Micro rotation profiles against M with $K = 0.5$, $m = 1$, Pr $= 0.71$, $\alpha = \pi/6$, $Kc = 1$, Gr $= 3$, Gm $= 2$, Sc $= 0.22$, $n = \pi/6$, $\Delta = 0.1$, $S = 1$, $F = 0.2$, $Q = 1$, $Q_1 = 0.2$

N_1 reduce, N_2 increase. The effects due to permeability of the porous parameter (K) on micro-rotational velocity are shown in Fig. 13. It is observed that as the permeability parameter increases, the micro-rotational velocity components N_1 decrease and N_2 increase in the entire flow field. As the Prandtl number Pr increases, the micro-rotational velocity components N_1 increase and N_2 reduce in the entire region of the fluid medium (Fig. 14). In Fig. 15, we found that the velocity component N_1 increase and N_2 decrease with increasing Schmidt number Sc. We also observed that the velocity component N_1 reduce and N_2 increase with increasing suction parameter S, viscosity ratio Δ and additional heat source Q, as seen in Figs. 16–18.

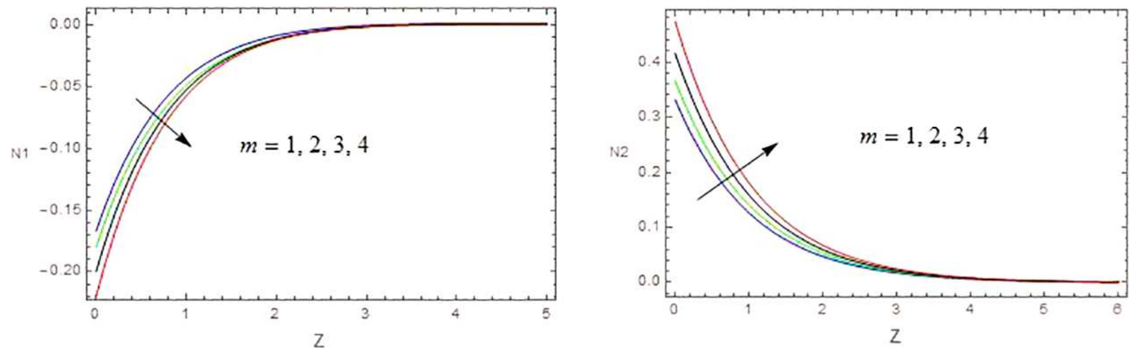

FIG. 12: Micro rotation profiles against m with $M = 0.5$, $K = 0.5$, $\Pr = 0.71$, $\alpha = \pi/6$, $Kc = 1$, $\text{Gr} = 3$, $\text{Gm} = 2$, $\text{Sc} = 0.22$, $n = \pi/6$, $\Delta = 0.1$, $S = 1$, $F = 0.2$, $Q = 1$, $Q_1 = 0.2$

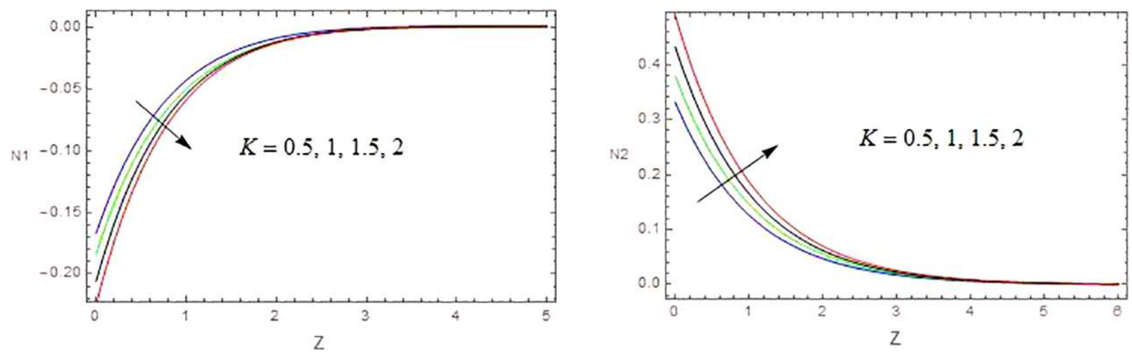

FIG. 13: Micro rotation profiles against K with $M = 0.5$, $m = 1$, $\Pr = 0.71$, $\alpha = \pi/6$, $Kc = 1$, $\text{Gr} = 3$, $\text{Gm} = 2$, $\text{Sc} = 0.22$, $n = \pi/6$, $\Delta = 0.1$, $S = 1$, $F = 0.2$, $Q = 1$, $Q_1 = 0.2$

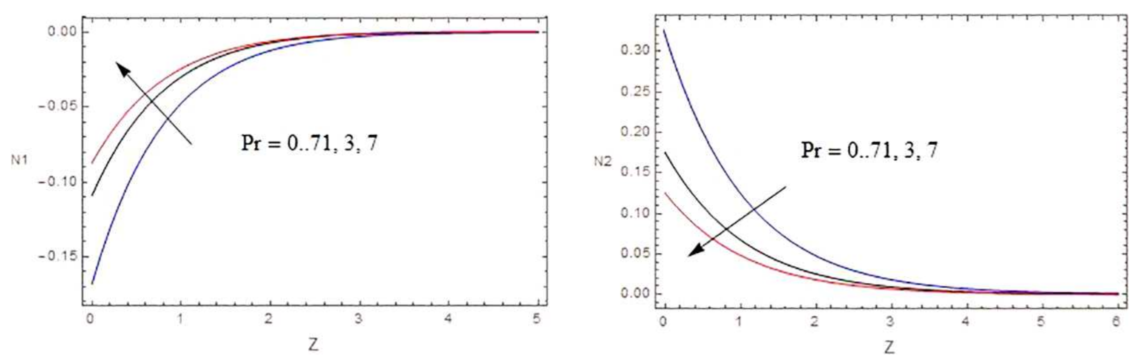

FIG. 14: Micro rotation profiles against Pr with $M = 0.5$, $K = 0.5$, $m = 1$, $\alpha = \pi/6$, $Kc = 1$, $\text{Gr} = 3$, $\text{Gm} = 2$, $\text{Sc} = 0.22$, $n = \pi/6$, $\Delta = 0.1$, $S = 1$, $F = 0.2$, $Q = 1$, $Q_1 = 0.2$

We also observed that an increase in Schmidt number Sc leads to reduced temperature (Fig. 19). The temperature decreases with increasing suction parameter S and Schmidt parameter Sc. The resultant temperature is raised with increasing radiation absorption parameter Q_1 and heat radiation parameter F in the entire flow region.

Figure 20 exhibits the resultant concentration with respect to the governing parameters Schmidt number Sc, suction parameter S, and chemical reaction parameter Kc, and is reduced with increasing Schmidt number Sc, suction parameter S, and chemical reaction parameter Kc. The fluid motion is retarded due to chemical reactions. Hence, the consumption of chemical species causes a fall in the concentration field, which in turn diminishes the buoyancy effects due to concentration gradients. Hence the flow field is retarded. Due to chemical reactions, the concentration

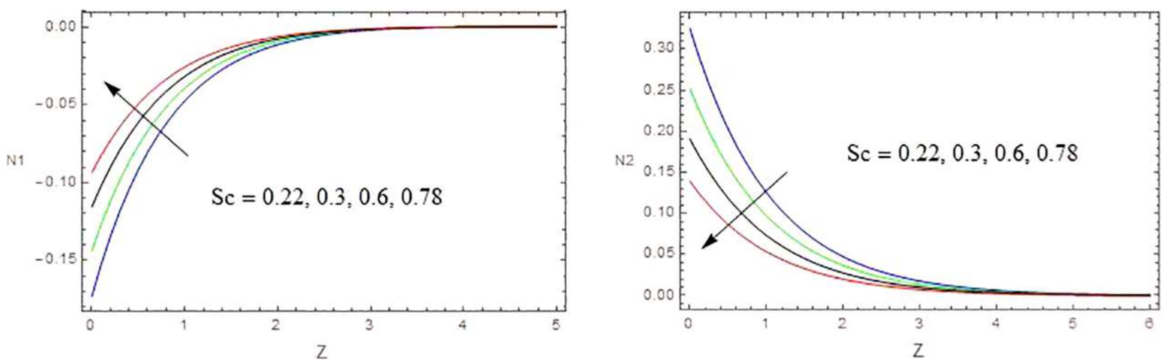

FIG. 15: Micro rotation profiles against Sc with $M = 0.5$, $K = 0.5$, $m = 1$, Pr $= 0.71$, $\alpha = \pi/6$, $Kc = 1$, Gr $= 3$, Gm $= 2$, $n = \pi/6$, $\Delta = 0.1$, $S = 1$, $F = 0.2$, $Q = 1$, $Q_1 = 0.2$

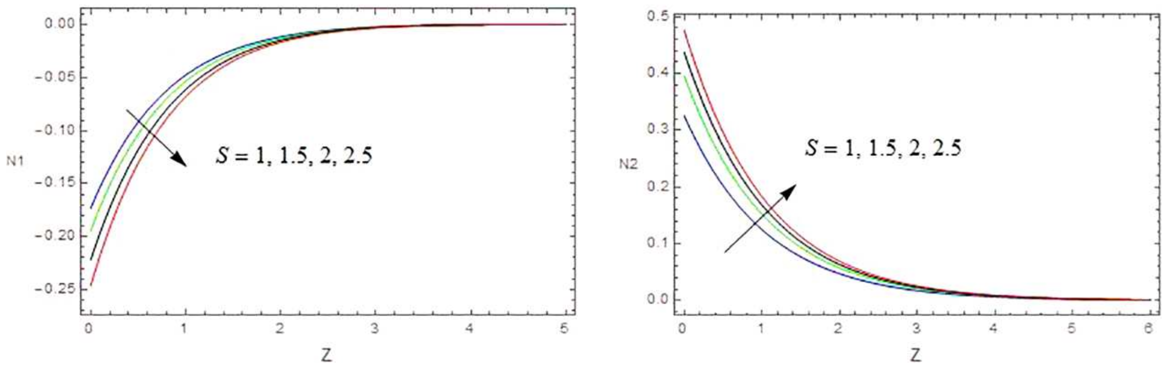

FIG. 16: Micro rotation profiles against S with $M = 0.5$, $K = 0.5$, $m = 1$, Pr $= 0.71$, $\alpha = \pi/6$, $Kc = 1$, Gr $= 3$, Gm $= 2$, Sc $= 0.22$, $n = \pi/6$, $\Delta = 0.1$, $F = 0.2$, $Q = 1$, $Q_1 = 0.2$

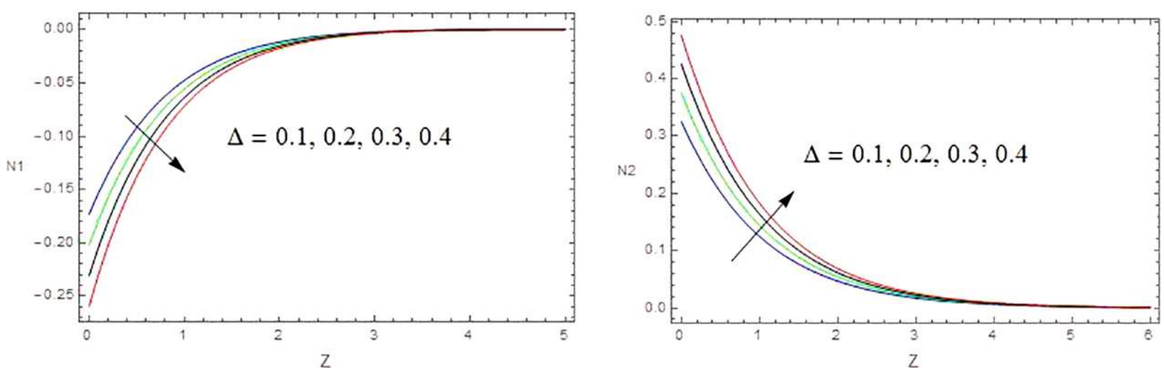

FIG. 17: Micro rotation profiles against S with $M = 0.5$, $K = 0.5$, $m = 1$, Pr $= 0.71$, $\alpha = \pi/6$, $Kc = 1$, Gr $= 3$, Gm $= 2$, Sc $= 0.22$, $n = \pi/6$, $S = 1$, $F = 0.2$, $Q = 1$, $Q_1 = 0.2$

of the fluid decreases. This is due to the dominate role of the Hall current and radiation absorption in the flow field.

Table 1 shows that the skin friction C_f and couple stress coefficient C_s both are upsurges with increasing heat radiation parameter F, Grashof number Gr, frequency of oscillation n. The skin friction C_f and couple stress coefficient C_s both are reduced with increasing magnetic field parameter M and Pr Prandtl number. We also noticed that with an increase in mass Grashof number Gm and viscosity ratio Δ, the skin friction C_f is increased and the couple stress coefficient C_s is decreased. It is observed from Table 1 that the skin friction C_f is decreased and the couple

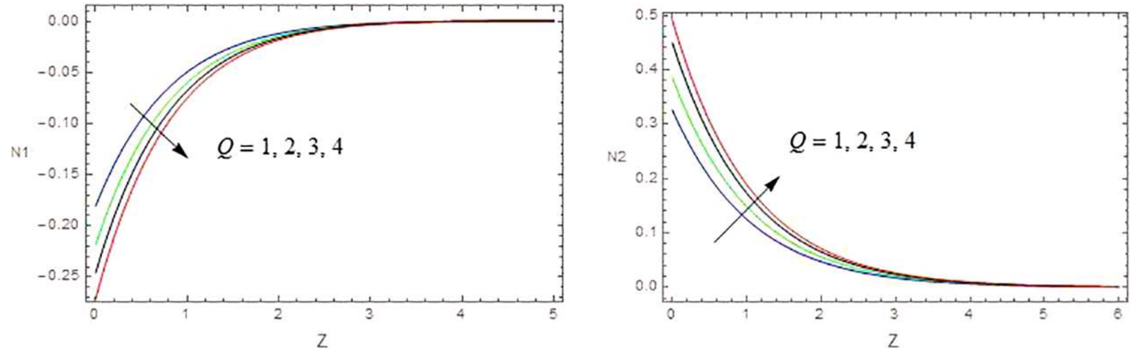

FIG. 18: Micro rotation profiles against Q with $M = 0.5$, $K = 0.5$, $m = 1$, $\Pr = 0.71$, $\alpha = \pi/6$, $Kc = 1$, $\mathrm{Gr} = 3$, $\mathrm{Gm} = 2$, $\mathrm{Sc} = 0.22$, $n = \pi/6$, $\Delta = 0.1$, $S = 1$, $F = 0.2$, $Q_1 = 0.2$

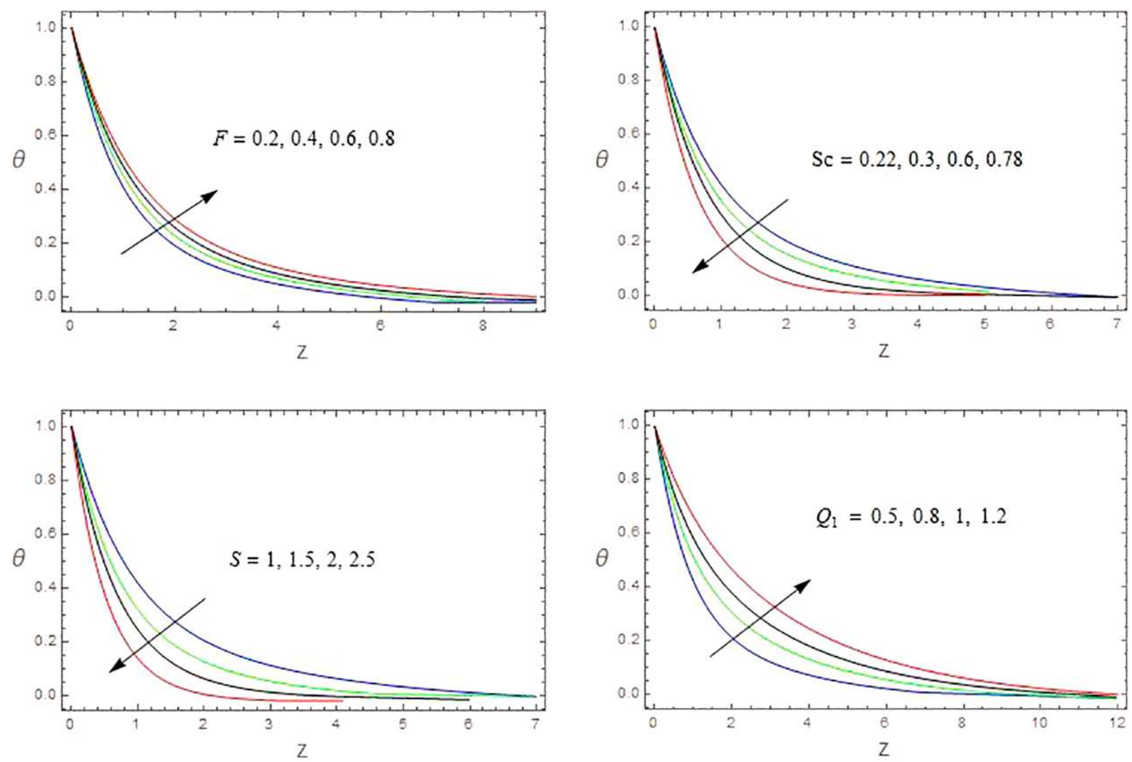

FIG. 19: Temperature profiles against F, Sc, S, Q_1

stress coefficient C_s is increased with increases in Hall current parameter m, permeability parameter K, Schmidt number Sc, suction parameter S, and chemical reaction parameter Kc.

Table 2 illustrates how the rate of heat transfer from the walls to the fluid is influenced by governing parameters Pr, Q, F, Sc, α, and Q_1. The surface heat transfer decreases with the increasing values of Prandtl number Pr, additional heat source parameter Q, heat radiation parameter F, and radiation absorption parameter Q_1, and also amplified with increasing in suction parameter S, Schmidt number Sc, and chemical reaction parameter Kc.

Table 3 shows the effects of Sc, S, and α on Sherwood number Sh_x. The rate of mass transfer increases with increasing parameters Schmidt number Sc or suction parameter S and/or chemical reaction parameter Kc.

To verify the validity and accuracy of the present analysis, we have compared our results of the velocity and micro-rotation velocity with those of Das (2011). It can be seen in Table 4 that excellent agreement between the

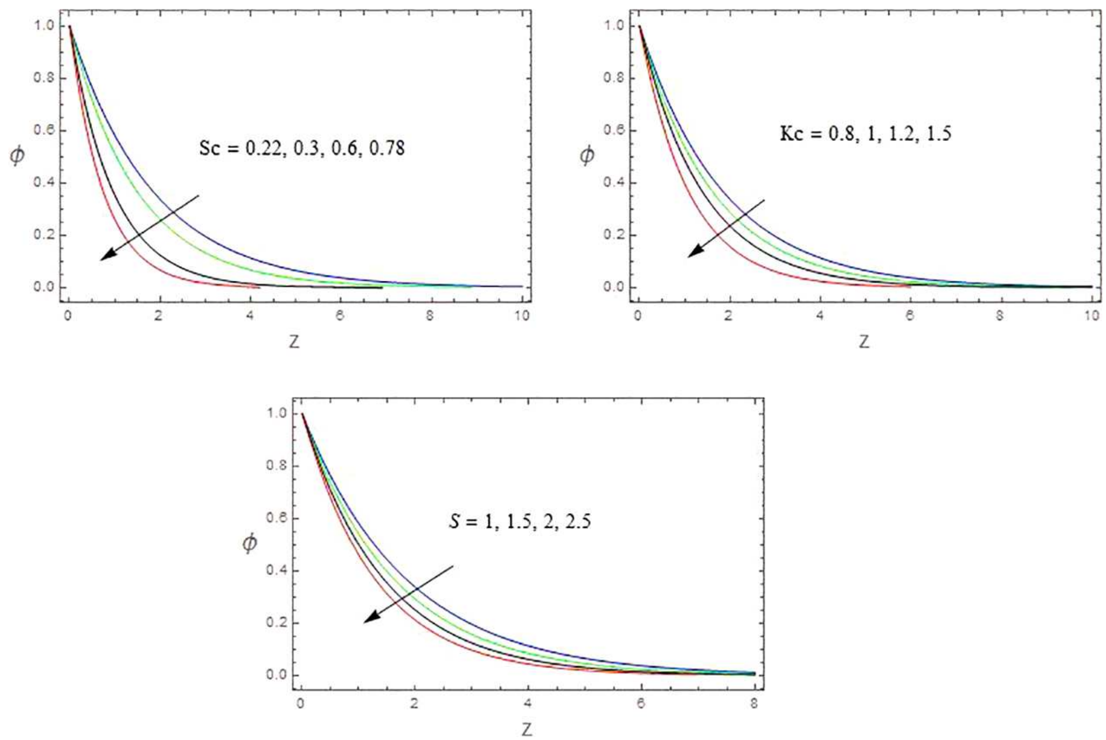

FIG. 20: Concentration profiles against Sc, Kc, and S

results exists. In addition, we observed that the fluid velocity and micro-rotations are lower for polar fluids than for Newtonian fluids.

4. CONCLUSIONS

We have studied the effects of heat and mass transfer on free convective flow of micropolar fluid over an infinite vertical porous plate in the presence of an inclined magnetic field with a constant suction velocity, taking Hall current into account. We conclude the following:

1. The resultant velocity reduces with increasing the intensity of the magnetic field, whereas it is enhanced with Hall parameter and additional heat source parameter.

TABLE 1: Frictional force and couple stress co-efficient

Pr	M	F	Sc	α	m	K	S	n	Δ	Gr	Gm	C_f	C_s
0.71	0.5	0.2	0.22	0.1	1	0.5	1	$\pi/6$	0.1	3	2	7.72490	0.959222
3	—	—	—	—	—	—	—	—	—	—	—	6.39235	0.705276
7	—	—	—	—	—	—	—	—	—	—	—	5.46917	0.493813
—	1	—	—	—	—	—	—	—	—	—	—	7.59040	0.962888
—	1.5	—	—	—	—	—	—	—	—	—	—	7.71676	0.968981
—	—	0.4	—	—	—	—	—	—	—	—	—	7.89635	0.995991
—	—	0.6	—	—	—	—	—	—	—	—	—	8.09145	1.024970
—	—	—	0.3	—	—	—	—	—	—	—	—	7.34894	0.977484
—	—	—	0.6	—	—	—	—	—	—	—	—	6.32507	1.002390

TABLE 1: *(continued)*

Pr	M	F	Sc	α	m	K	S	n	Δ	Gr	Gm	C_f	C_s
—	—	—	—	0.3	—	—	—	—	—	—	—	7.27434	0.987946
—	—	—	—	0.5	—	—	—	—	—	—	—	7.10875	1.010820
—	—	—	—	—	2	—	—	—	—	—	—	7.67192	0.960650
—	—	—	—	—	3	—	—	—	—	—	—	7.68135	0.961925
—	—	—	—	—	—	1	—	—	—	—	—	6.35897	1.085790
—	—	—	—	—	—	2	—	—	—	—	—	5.73926	1.154850
—	—	—	—	—	—	—	1.5	—	—	—	—	7.40204	1.497690
—	—	—	—	—	—	—	2	—	—	—	—	7.04974	2.095500
—	—	—	—	—	—	—	—	$\pi/4$	—	—	—	8.18970	1.120600
—	—	—	—	—	—	—	—	$\pi/3$	—	—	—	7.98877	1.282000
—	—	—	—	—	—	—	—	—	0.2	—	—	9.75657	0.913276
—	—	—	—	—	—	—	—	—	0.3	—	—	10.1281	0.872901
—	—	—	—	—	—	—	—	—	—	4	—	10.5851	1.386850
—	—	—	—	—	—	—	—	—	—	5	—	13.2342	1.814490
—	—	—	—	—	—	—	—	—	—	—	3	8.57907	0.876479
—	—	—	—	—	—	—	—	—	—	—	4	9.01739	0.793736

TABLE 2: Nusselt number

S	Pr	Q	F	Sc	α	Q_1	Nu
0	0.71	1	0.2	0.22	0.1	0.5	0.618220
1	—	—	—	—	—	—	0.915702
2	—	—	—	—	—	—	1.323740
—	3	—	—	—	—	—	-0.253603
—	6	—	—	—	—	—	-1.395730
—	—	2	—	—	—	—	-0.429284
—	—	3	—	—	—	—	0.135285
—	—	—	0.4	—	—	—	0.565369
—	—	—	0.6	—	—	—	0.522467
—	—	—	—	0.3	—	—	0.624555
—	—	—	—	0.6	—	—	0.641263
—	—	—	—	—	0.3	—	0.643843
—	—	—	—	—	0.5	—	0.658834
—	—	—	—	—	—	1	0.347917
—	—	—	—	—	—	1.5	0.077613

2. The micro-rotational velocity increases with increasing Hall parameter.
3. Temperature increases with increasing heat radiation parameter and reduces with suction parameter.
4. Concentration reduces with increasing chemical reaction parameter.
5. The magnitude of skin friction at the plate decreases, due to increasing Hartmann number, frequency of oscillation, and heat radiation parameter.
6. The magnitude of couple stress coefficient increases with chemical reaction parameter and reduces with mass Grashof number.

TABLE 3: Sherwood number

Sc	S	α	Sh_x
0.22	1	0.1	0.294662
0.3	—	—	0.379129
0.6	—	—	0.687298
—	3	—	0.48533
—	2	—	0.691801
—	—	0.3	0.389464
—	—	0.5	0.459428

TABLE 4: Comparison of results Pr $= 0.71$, $\alpha = 0.1$, Gr $= 3$, Gm $= 2$, Sc $= 0.22$, $n = \pi/6$, $\Delta = 0.1$, $S = 1$, $F = 0.2$, $Q = 1$, $\varepsilon = 0.01$, $t = 1$, and $z = 0.5$

M	K	Previous Results Das (2011) for velocity u	Present results $m = 0$, $Q_1 = 0$ for velocity u	Previous Results Das (2011) for micro-rotational velocity N_1	Present results $m = 0$, $Q_1 = 0$ for micro-rotational velocity N_1
0.5	0.5	2.75120	2.75118	–0.0640853	–0.0640841
1	—	2.74854	2.74851	–0.0640141	–0.0640098
1.5	—	2.73493	2.73488	–0.0638959	–0.0638899
2	—	2.72830	2.72826	–0.0637317	–0.0637288
—	1	2.86682	2.86678	–0.0772872	–0.0772788
—	2	3.48735	3.48731	–0.0894623	–0.0894597
—	3	3.99979	3.99975	–0.0955901	–0.0955874

7. The rate of heat transfer increase due to increase in suction parameter reduces with Prandtl number.

8. The rate of mass transfer is enhanced with Schmidt number, suction parameter and chemical reaction parameter.

REFERENCES

Abo-Eldohad, E.M. and Ghonaim, A.F., Radiation Effect on Heat Transfer of a Micro-Polar Fluid through a Porous Medium, *Appl. Math. Comput.*, vol. **169**, no. 1, pp. 500–516, 2005.

Ahmed, N. and Kalita, D., Transient MHD Free Convection from an Infinite Vertical Porous Plate in a Rotating System with Mass Transfer and Hall Current, *J. Energy Heat Mass Transf.*, vol. **33**, pp. 271–292, 2011.

Ariman, T., Turk, M.A., and Sylvester, N.D., Micro-Continuum Fluid Mechanics—A Review, *Int. J. Eng. Sci.*, vol. **11**, pp. 905–930, 1973.

Bakr, A.A., Effects of Chemical Reaction on MHD Free Convection and Mass Transfer Flow of a Micro-Polar Fluid with Oscillatory Plate Velocity and Constant Heat Source in a Rotating Frame of Reference, *Comm. Nonlinear Sci. Numer. Simul.*, vol. **16**, pp. 698–710, 2011.

Bhargava, R., Anwar Beg, O., Sharma, S., and Zueco, J., Finite Element Study of Nonlinear Two-Dimensional Deoxygenated Bio-Magnetic Micro-Polar Flow, *Comm. Nonlinear Sci. Numer. Simul.*, vol. **15**, no. 15, pp. 1210–1223, 2010.

Chakraborti, A., Gupta, A.S., Das, B.K., and Jana, R.N., Hydromagnetic Flow past a Rotating Porous Plate in a Conducting Fluid Rotating about a Non-Coincident Parallel Axis, *Acta Mech.*, vol. **176**, pp. 107–119, 2005.

Chamkha, A.J., Mohamed, R.A., and Ahmed, S.E., Unsteady MHD Natural Convection from a Heated Vertical Porous Plate in a Micropolar Fluid with Joule Heating, Chemical Reaction and Radiation Effects, *Meccanica*, vol. **46**, pp. 399–411, 2011.

Damseh, R.A., Al-Odat, M.Q., Chamkha, A.J., and Benbella Shannk, A., Combined Effect of Heat Generation/Absorption and

First Order Chemical Reaction on Micro-Polar Fluid Flows over a Uniform Stretched Permeable Surface, *Int. J. Therm. Sci.*, vol. **48**, pp. 1658–1663, 2009.

Das, K., Effect of Chemical Reaction and Thermal Radiation on Heat and Mass Transfer Flow of MHD Micro-Polar Fluid in a Rotating Frame of Reference, *Int. J. Heat Mass Transf.*, vol. **54**, nos. 15-16, pp. 3505–3513, 2011. DOI: 10.1615/SpecialTopicsRevPorousMedia.2018022792

Eringen, A.C., Simple Micro Fluids, *Int. J. Eng. Sci.*, vol. **2**, pp. 205–217, 1964.

Eringen, A.C., Theory of Thermomicrofluids, *J. Math Anal. Appl.*, vol. **38**, pp. 480–496, 1972.

Ezzat, M.A. and Othman, I.A.M., Thermal Instability in a Rotating Micro-Polar Fluid Layer Subject to an Electric Field, *Int. J. Eng. Sci*., vol. **38**, pp. 1851–1867, 2000.

Ezzat, M.A., Othman, I.A.M., and Helmy, K.A., A Problem of a Micro-Polar Magnetohydrodynamic Boundary Layer Flow, *Can. J. Phys*., vol. **77**, pp. 813–827, 1999.

Fu, Q., Du, Z., and Wang, S., The Study on the Distribution Law of Interwell Pressure Gradient Considering the Influence of Profile Control and Water Shutoff, *J. Porous Media*, vol. **21**, no. 3, pp. 241–256, 2018. DOI: 10.1615/JPorMedia.v21.i3.40

Ganapathy, R., A Note on Oscillatory Couette Flow in a Rotating System, *ASME J. Appl. Mech.*, vol. **61**, pp. 208–209, 1994.

Hayat, T., Khan, S.B., Sajid, M., and Asghar, S., Rotating Flow of a Third Grade Fluid in a Porous Space with Hall Current, *Nonlinear Dyn*., vol. **49**, pp. 83–91, 2007.

Hickman, K.C.D., Centrifugal Boiler Compression Still, *Ind. Eng Chem*., vol. **49**, pp. 786–800, 1957.

Ibrahim, F.S., Elaiw, A.M., and Bakr, A.A., Effect of the Chemical Reaction and Radiation Absorption on the Unsteady MHD Free Convection Flow past a Semi-Infinite Vertical Permeable Moving Plate with Heat Source and Suction, *Commun. Nonlinear Sci. Numer. Simul.*, vol. **13**, no. 6, pp. 1056–1066, 2008.

Kaothekar, S., Thermal Instability of Partially Ionized Viscous Plasma with Hall Effect FLR Corrections Flowing through Porous Medium, *J. Porous Media*, vol. **21**, no. 8, pp. 679–699, 2018. DOI: 10.1615/JPorMedia.2018017559

Mahmoud, M.A.A., Thermal Radiation Effects on MHD Flow of a Micropolar Fluid over a Stretching Surface with Variable Thermal Conductivity, *Physica A.*, vol. **375**, pp. 401–410, 2007.

Mazumder, B.S., An Exact Solution of Oscillatory Couette Flow in a Rotating System, *ASME J. Appl. Mech*., vol. **58**, no. 4, pp. 1104–1107, 1991.

Mohsen, N., Mahmoudi, M., Aghdasi, M., and Tamayol, A., Heat Transfer Cartography from a Hot Elliptical Cylinder Wrapped with a Porous Medium, *J.Porous Media*, vol. **20**, no. 12, pp. 1119–1135, 2017. DOI: 10.1615/JPorMedia.v20.i12.50

Muthuraj, R. and Srinivas, S., Fully Developed MHD Flow of a Micro-Polar and Viscous Fluids in a Vertical Porous Space using HAM, *Int. J. Appl. Math Mech.*, vol. **6**, no. 11, pp. 55–78, 2010.

Othman, I.A.M. and Zaki, S.A., Thermal Relaxation Effect on Magnetohydrodynamic Instability in a Rotating Micropolar Fluid Layer Heated from Below, *Acta Mech*., vol. **170**, nos. 1-4, pp. 187–197, 2004.

Othman, I.A.M. and Zaki, S.A., Thermal Instability in a Rotating Micropolar Viscoelastic Fluid Layer under the Effect of Electric Field, *Mech. Mech. Eng.*, vol. **12**, no. 2, pp. 171–184, 2008.

Prathap Kumar, J., Umavathi, J.C., Chamkha, A.J., and Pop I., Fully Developed Free Convective Flow of Micro-Polar and Viscous Fluids in a Vertical Channel, *Appl. Math. Model*., vol. **34**, pp. 1175–1186, 2010.

Rahman, M.M. and Al-Lawatia, M., Effect of Higher Order Chemical Reaction on Micro-Polar Fluid Flow on a Power Law Permeable Stretched Sheet with Variable Concentration in a Porous Medium, *Can. J. Chem. Eng*., vol. **88**, pp. 23–32, 2010.

Rahman, M.M. and Sultana, T., Radiative Heat Transfer Flow of Micropolar Fluid with Variable Heat Flux in a Porous Medium, *Nonlinear Anal. Model. Control*., vol. **13**, no. 1, pp. 71–87, 2008.

Rahman, M.M., Aziz, A., and Al-Lawatia, M., Heat Transfer in Micro-Polar Fluid along an Inclined Permeable Plate with Variable Fluid Properties, *Int. J. Therm. Sci.*, vol. **49**, pp. 993–1002, 2010.

Rani, N. and Tomar, S.K., Thermal Convection Problem of Micro-Polar Fluid Subjected to Hall Current, *Appl. Math. Model.*, vol. **34**, pp. 508–519, 2010.

Reddy, B.S.K., Veera Krishna, M., Rao, K.V.S.N., and Bhuvana Vijaya, R., HAM Solutions on MHD Flow of Nano-Fluid through Saturated Porous Medium with Hall Effects, *Mater. Today: Proc.*, vol. **5**, pp. 120–131, 2018. DOI: 10.1016/j.matpr.2017.11.062

Sarifuddin, Chakravarty, S., and Mandal, P.K., Heat Transfer to Micropolar Fluid Flowing through an Irregular Arterial Constriction, *Int. J. Heat Mass Transf.*, vol. **56**, pp. 338–351, 2013.

Satya Narayana, P.V., Rami Reddy, G., and Venkataramana, S., Hall Current Effects on Free-Convection MHD Flow past a Porous Plate, *Int. J. Automot. Mech. Eng.*, vol. **3**, pp. 350–363, 2011.

Satya Narayana, P.V., Venkateswarlu, B., and Venkataramana, S., Effects of Hall Current and Radiation Absorption on MHD Micropolar Fluid in a Rotating System, *Ain Shams Engin. J.*, vol. **4**, pp. 843–854, 2013.

Sharma, K. and Gupta, S., Radiation Effects on MHD Boundary Layer Flow and Heat Transfer along a Stretching Cylinder with Variable Thermal Conductivity in a Porous Medium, *J. Porous Media*, vol. **21**, no. 8, pp. 763–779, 2018. DOI: 10.1615/JPorMedia.2018019284

Shercliff, J.A., *A Text Book of Magnetohydrodynamics*, New York: Pergamon Press Inc., 1965.

Sivaraj, R. and Rushi Kumar, B., Chemically Reacting Dusty Visco-Elastic Fluid Flow in an Irregular Channel with Convective Boundary, *Ain Shams Eng. J.*, vol. **4**, pp. 93–101, 2012.

Sravan Kumar, T. and Rushi Kumar, B., Magnetohydrodynamic Nanofluid Flow and Heat Transfer over a Stretching Sheet, *Special Topics Rev. Porous Media: Int. J.*, vol. **9**, no. 4, pp. 365–378, 2018. DOI: 10.1615/SpecialTopicsRevPorousMedia.2018022792

Srinivasacharya, D., Ramanamurthy, J.V., and Venugopalam, D., Unsteady Stoke's Flow of Micro-Polar Fluid between two Parallel Porous Plates, *Int. J. Eng Sci*., vol. **39**, pp. 1557–1563, 2001.

Sudheer Babu, M. and Satya Narayana, P.V., Effects of the Chemical Reaction and Radiation Absorption on Free Convection Flow through Porous Medium with Variable Suction in the Presence of Uniform Magnetic Field, *J. Heat Mass Transf.*, vol. **3**, pp. 219–234, 2009.

Swarnalathamma, B.V. and Veera Krishna, M., Peristaltic Hemodynamic Flow of Couple Stress Fluid through a Porous Medium under the Influence of Magnetic Field with Slip Effect, *AIP Conf. Proc.*, vol. **1728**, p. 020603, 2016. DOI: 10.1063/1.4946654

Umavathi, J.C. and Malashetty, M.S., Magnetohydrodynamic Mixed Convection in a Vertical Channel, *Int. J. Non-Linear Mech.*, vol. **40**, pp. 91–101, 2005.

Veera Krishna, M. and Chamkha, A.J., Hall Effects on Unsteady MHD Flow of Second Grade Fluid through Porous Medium with Ramped Wall Temperature and Ramped Surface Concentration, *Phys. Fluids*, vol. **30**, p. 053101, 2018. DOI: 10.1063/1.5025542

Veera Krishna, M. and Gangadhar Reddy, M., MHD Free Convective Boundary Layer Flow through Porous Medium past a Moving Vertical Plate with Heat Source and Chemical Reaction, *Mater. Today: Proc.*, vol. **5**, pp. 91–98, 2018. DOI: 10.1016/j.matpr.2017.11.058

Veera Krishna, M. and Gangadhar Reddy, M., MHD Free Convective Rotating Flow of Visco-Elastic Fluid past an Infinite Vertical Oscillating Porous Plate with Chemical Reaction, *IOP Conf. Series: Mat. Sci. Eng.*, vol. **149**, p. 012217, 2016. DOI: 10.1088/1757-899X/149/1/012217

Veera Krishna, M. and Jyothi, K., Hall Effects on MHD Rotating Flow of a Visco-Elastic Fluid through a Porous Medium over an Infinite Oscillating Porous Plate with Heat Source and Chemical Reaction, *Materials Today: Proc.*, vol. **5**, pp. 367–380, 2018a. DOI: 10.1016/j.matpr.2017.11.094

Veera Krishna, M. and Jyothi, K., Heat and Mass Transfer on MHD Rotating Flow of a Visco-Elastic Fluid through Porous Medium with Time Dependent Oscillatory Permeability, *J. Anal.*, vol. **25**, no. 2, pp. 1–19, 2018b. DOI: 10.1007/s41478-018-0099-0

Veera Krishna, M. and Subba Reddy, G., MHD Forced Convective Flow of Non-Newtonian Fluid through Stumpy Permeable Porous Medium, *Materials Today: Proc.*, vol. **5**, pp. 175–183, 2018a. DOI: 10.1016/j.matpr.2017.11.069

Veera Krishna, M. and Subba Reddy, G., Unsteady MHD Reactive Flow of Second Grade Fluid through Porous Medium in a Rotating Parallel Plate Channel, *J. Anal*., vol. **25**, no. 2, pp. 1–19, 2018b. DOI: 10.1007/s41478-018-0108-3

Veera Krishna, M. and Subba Reddy, B., Unsteady MHD Convective Flow of Second Grade Fluid through a Porous Medium in a Rotating Parallel Plate Channel with Temperature Dependent Source, *IOP Conf. Series: Mat. Sci. Eng.*, vol. **149**, p. 012216, 2016. DOI: 10.1088/1757-899X/149/1/012216

Veera Krishna, M. and Swarnalathamma, B.V., Convective Heat and Mass Transfer on MHD Peristaltic Flow of Williamson Fluid with the Effect of Inclined Magnetic Field, *AIP Conf. Proc.*, vol. **1728**, p. 020461, 2016. DOI: 10.1063/1.4946512

Veera Krishna, M., Gangadhara Reddy, M., and Chamkha, A.J., Heat and Mass Transfer on MHD Free Convective Flow over an Infinite Non-Conducting Vertical Flat Porous Plate, *Int. J. Fluid Mech. Res*., vol. **45**, no. 5, pp. 1–25, 2018d. DOI: 10.1615/InterJFluidMechRes.2018025004

Veera Krishna, M., Gangadhar Reddy, M., and Chamkha, A.J., Heat and Mass Transfer on Non-Linear MHD Flow through Oscillating Infinite Vertical Porous Surface, *J. Porous Media*, vol. **21**, 2018f (in press).

Veera Krishna, M., Jyothi, K., and Chamkha, A.J., Heat and Mass Transfer on MHD Flow of Second Grade Fluid through Porous Medium over a Semi-Infinite Vertical Stretching Sheet, *J. Porous Media*, vol. **21**, 2018g. (in press).

Veera Krishna, M., Jyothi, K., and Chamkha, A.J., Heat and Mass Transfer on Unsteady, Magnetohydrodynamic Oscillatory Flow of Second-Grade Fluid through a Porous Medium between Two Vertical Plates, under the Influence of Fluctuating Heat Source/Sink, and Chemical Reaction, *Int. J. Fluid Mech. Res.*, vol. **45**, no. 5, pp. 459–477, 2018c. DOI: 10.1615/InterJFluidMechRes.2018024591

Veera Krishna, M., Prasad, R.S., and Krishna, D.V., Hall Effects on Steady Hydromagnetic Flow of a Couple Stress Fluid through a Composite Medium in a Rotating Parallel Plate Channel with Porous Bed on the Lower Half, *Adv. Studies Contemp. Math. (Kyungshang)*, vol. **20**, no. 3, pp. 457–468, 2010.

Veera Krishna, M., Subba Reddy, G., and Chamkha, A.J., Hall Effects on Unsteady MHD Oscillatory Free Convective Flow of Second Grade Fluid through Porous Medium between Two Vertical Plates, *Phys. Fluids*, vol. **30**, p. 023106, 2018b. DOI: 10.1063/1.5010863

Veera Krishna, M., Swarnalathamma, B.V., and Chamkha, A.J., Heat and Mass Transfer on Magnetohydrodynamic Chemically Reacting Flow of Micropolar Fluid through a Porous Medium with Hall Effects, *Special Topics Rev. Porous Media: Int. J.*, vol. **9**, no. 4, pp. 347–364, 2018e. DOI: 10.1615/SpecialTopicsRevPorousMedia.2018024579

Veera Krishna, M., Swarnalathamma, B.V., and Prakash, J., Heat and Mass Transfer on Unsteady MHD Oscillatory Flow of Blood through Porous Arteriole, *Appl. Fluid Dynamics, Lecture Notes Mech. Eng.*, vol. **XXII**, pp. 207–224, 2018a.

Wu, Y., Zou, Z., Fu, C., and Zhang, W., Numerical Study of Porous Blunt Nosecone Transpiration Cooling under Supersonic Incoming Flow, *J. Porous Media*, vol. **20**, no. 7, pp. 607–618, 2017. DOI: 10.1615/JPorMedia.v20.i7.30